

Life after eruption – III. Orbital periods of the old novae V365 Car, AR Cir, V972 Oph, HS Pup, V909 Sgr, V373 Sct and CN Vel

C. Tappert,^{1*} L. Schmidtobreick,² N. Vogt,¹ and A. Ederoclite³ *†

¹*Departamento de Física y Astronomía, Universidad de Valparaíso, Avda. Gran Bretaña 1111, 2360102 Valparaíso, Chile*

²*European Southern Observatory, Alonso de Cordova 3107, 7630355 Santiago, Chile*

³*Centro de Estudios de Física del Cosmos de Aragón, Plaza San Juan 1, Planta 2, Teruel, E44001, Spain*

Accepted. Received

ABSTRACT

We present time-series photometric and spectroscopic data for seven old novae. They are used to derive the orbital period for the systems V365 Car (5.35 h), AR Cir (5.14 h), V972 Oph (6.75 h), HS Pup (6.41 h), V373 Sct (3.69 h), V909 Sgr (3.43 h) and CN Vel (5.29 h). Their addition increases the number of orbital periods for novae by ~ 10 per cent. The eclipsing nature of V909 Sgr is confirmed, and in three other cases (V365 Car, Ar Cir and V373 Sct) we detect significant photometric orbital variability with amplitudes ≥ 0.2 mag in R . The resulting period distribution is briefly discussed. We furthermore provide new measurements for the previously ambiguous coordinates for AR Cir and CN Vel and the identification of a new probable W UMa variable in the field of V909 Sgr. The spectrum of V972 Oph presents an emission feature redward of $H\alpha$ which we tentatively identify with the CII $\lambda\lambda 6578/6583$ doublet. It is shown that this line originates in the binary and not in a shell, and to our knowledge this is the first time that it has been detected in such quality in a cataclysmic variable (CV). We argue that this line could be more common in CVs, but that it can be easily masked by the broad $H\alpha$ emission that is typical for these systems. A closer inspection of the line profiles of the other novae indeed reveals an extended red wing in V365 Car, CN Vel and AR Cir. In the latter system additionally an absorption counterpart blueward of $H\alpha$ is detected and thus in this case a bipolar outflow appears as a more likely scenario rather than CII emission.

Key words: binaries: close – binaries: eclipsing – novae, cataclysmic variables

1 INTRODUCTION

The intrinsic distribution of cataclysmic variables (CVs) is determined by two elements. First, there is the period distribution of newly formed CVs, i.e. the distribution of the periods at which the late-type secondary star starts to transfer mass on to the white dwarf primary via Roche lobe overflow for the first time. Secondly, there is the secular evolution of CVs from this period that is governed by continuous angular momentum loss due to magnetic braking and gravitational radiation, which decreases the binary separation and thus the orbital period for non-degenerate secondary stars (e.g., King 1988). As CVs that are born with periods $P_{\text{orb}} > 3$ h evolve below this point the secondary star becomes fully convective. It is generally thought that as a consequence magnetic braking stops to operate or at least becomes much less efficient, causing the system to become detached until it restarts mass transfer at $P_{\text{orb}} \sim 2$ h (Rappaport, Verbunt, & Joss 1983). The result is a

paucity of CVs with periods between ~ 2 and 3 h, the so-called period gap. Finally, the minimum period at ~ 80 min represents the turn-around point when the secondary star becomes degenerate and the CV now evolves, very slowly, back to longer orbital periods due to the inverted mass-radius relation. Modelling predicts that most CVs have orbital periods between ~ 80 min and 2 h (de Kool 1992; Stehle, Kolb, & Ritter 1997).

Although modern surveys have unveiled more of the intrinsic CV population (e.g., Gänsicke et al. 2009) the currently observed period distribution is still affected by a strong observational bias. The latter includes a mixture of factors, but the main contributors will be the brightness of the CV and frequency and amplitude of the variability. With increasing mass-transfer rate \dot{M} the amplitude of the dwarf nova outbursts decreases, but the frequency increases, and also the brightness of the accretion disc, which is the dominant light source in most CVs (e.g., Lasota 2001, and references therein). Since \dot{M} for systems above the gap exceeds the one for CVs below it by one to two orders of magnitude (Townsend & Gänsicke 2009), these are the objects that are favoured by the observational bias.

Classical novae are CVs that undergo a thermonuclear ex-

* E-mail: claus.tappert@uv.cl

† Based on observations with ESO telescopes, proposal numbers 083.D-0158(A), 086.D-0428(A), 087.D-0323(A), 088.D-0588(A), 089.D-0505(C)

plosion on the surface of the white dwarf due to the accreted mass having reached a critical value (Starrfield, Sparks, & Truran 1976). The underlying binary is not destroyed by the nova eruption and mass transfer is reestablished on time-scales not longer than one or two years (e.g., Retter, Leibowitz, & Kovo-Kariti 1998). Nova eruptions can thus be assumed to be recurrent events. The recurrence time in classical novae is estimated to be $t_{\text{rec}} > 10^3$ yr (Shara et al. 2012a). While it is not yet entirely clear how strongly other parameters like magnetic fields or the chemical compositions affect t_{rec} , the most important factors have been shown to be \dot{M} , the internal temperature of the white dwarf T_c and its mass M_{WD} . However, M_{WD} is mainly independent of P_{orb} (Zorotovic, Schreiber, & Gänsicke 2011), and while Nelson, MacCannell, & Dubeau (2004) have shown that T_c is an important factor in the shaping of the orbital period distribution, Townsley & Bildsten (2004) find that T_c depends on the long-term average \dot{M} . It is thus reasonable to assume that the latter represents the overall most important factor for the nova period distribution. Since the highest values for \dot{M} are found in CVs with $P_{\text{orb}} \sim 3 - 4$ h (Townsley & Gänsicke 2009), one would expect that the observed period distribution for novae shows a strong maximum at such periods. Detailed calculations by Townsley & Bildsten (2005) show that roughly 50 per cent of the novae should have orbital periods in this range. Diaz & Bruch (1997) analyse the influence of several observational selection effects, but find that they do not strongly affect the overall shape of the period distribution.

The main problem with comparing theoretically derived period distributions to the actually observed one is that the latter is still significantly undersampled. The current edition of the Ritter & Kolb (2003) catalogue (update 7.20) lists only 69 post-novae with unambiguous periods. The problem of undersampling extends to all aspects of post-nova research, which motivated us to start a project to select candidates for ‘lost’ post-novae via colour-colour diagrams, to confirm the post-nova spectroscopically, and to derive the orbital period for suitable, i.e. sufficiently bright systems (Tappert et al. 2012, 2013, hereafter Paper I, II). In the present paper we report on the orbital periods for seven post-novae.

2 DATA HANDLING

2.1 Observations and reduction

The time-series data were obtained on several observing runs in 2011 and 2012 at the ESO-NTT, La Silla, Chile, using EFOSC2 (Eckert, Hofstadt, & Melnick 1989). The meteorological conditions were not photometric, with the 2011 runs being strongly affected by clouds and poor seeing, while for the 2012 runs the sky was mostly clear with reasonably good seeing ~ 1.0 arcsec. Spectroscopy was performed with grism #20 and a 1 arcsec slit, yielding a wavelength range 6035–7135 Å at a spectral resolution of 3.8 Å, the latter measured as the full width at half-maximum (FWHM) of an arc line. Additional low-resolution spectroscopy with grism #4 and a 1 arcsec slit was taken in 2009 May for some of the systems. The corresponding wavelength range was 4000–7400 Å at a resolution of 11 Å. The acquisition of the targets was done by taking 10 or 20 s exposures of the field with a Bessel *R* filter (ESO #642). For one object (V909 Sgr), additionally a light curve was taken using a Bessel *V* filter (ESO #641). A detailed observing log is given in Table 1, stating the observing dates, the grism used, the number n of individual exposures in a specific night, the exposure time t_{exp} (for the grism #4 data this is the total exposure time), the time range

Table 1. Log of observations.

Object	Date	Grism (Å)	n	t_{exp} (s)	Δt (h)	R (mag)	
V365 Car	2011 February 26	#20	3	720	0.42	17.64	
	2011 February 27		3		0.42	17.60	
	2011 February 28		4	900	1.59	17.57	
	2011 March 01		1		–	17.61	
	2011 March 02		3		5.69	17.67	
	2011 March 03		4		5.83	17.64	
	2012 March 25		3		5.17	17.61	
	2012 March 26		4		5.11	17.73	
	2012 March 27		3		2.26	17.67	
	2012 March 28		19		5.45	17.68	
	2012 April 02		8		2.46	17.61	
	2012 May 15		14		4.06	17.69	
	2012 May 16		12		3.54	17.66	
	2012 May 17		5		2.01	17.69	
	2012 May 18		9		4.80	17.70	
	2012 May 19		6		4.06	17.68	
	AR Cir	2012 May 17	#20	6	900	3.11	17.66
		2012 May 18		7		7.45	17.76
		2012 May 19		4		2.44	17.75
V972 Oph	2011 June 30	#20	3	900	3.51	15.90	
	2011 July 01		7		9.44	15.93	
	2012 May 16		2		3.24	15.86	
	2012 May 17		2		0.77	15.72	
	2012 May 18		5		6.69	15.82	
HS Pup	2012 May 19		5		2.74	15.77	
	2009 May 19	#4	6	3570	–	17.59	
	2009 May 22		3	1260	–	17.62	
	2009 May 23		3	1890	–	17.66	
	2011 February 26	#20	6	720	2.07	17.89	
	2011 February 28		1		–	17.96	
	2011 March 01		3	900	2.21	17.88	
	2011 March 02		3		1.83	17.92	
V909 Sgr	2011 March 03		5		4.15	18.01	
	2012 May 16	#20	9	900	5.50	20.15	
	2012 May 17		6		1.62	20.03	
	2012 May 18		7		5.96	20.11	
	2012 May 19	<i>V</i>	175	60	4.74	20.46 ^a	
V373 Sct	2011 June 29	#20	4	900	6.40	18.82	
	2011 June 30		4	900	5.82	18.83	
	2011 July 01		5	900	6.94	18.63	
CN Vel	2009 May 19	#4	6	2160	–	17.48	
	2009 May 22		3	540	–	17.49	
	2009 May 23		3	540	–	17.43	
	2009 May 24		3	2100	–	17.45	
	2011 February 26	#20	3	750	0.44	17.56	
	2011 February 28		1	900	–	17.58	
	2011 March 01		3	900	3.28	17.53	
	2011 March 02		2	900	1.59	17.53	
2011 March 03		4	900	5.89	17.54		

a) *V* magnitude

Δt covered by the time-series observations and the average *R*-band magnitude during that night. For the photometric time-series data of V909 Sgr, the average *V* magnitude is given.

Data reduction was performed with IRAF. For the photometric data (the acquisition frames and the light curve for V909 Sgr), this included only the subtraction of bias frames, but no flat-field correction because EFOSC2 flats are affected by a central light concentration. Photometric magnitudes for all stars on the frames were extracted using IRAF’s DAOPHOT package and the standalone

DAOMATCH and DAOMASTER routines (Stetson 1992). The aperture radius for a given frame was chosen as a few tenths of a pixel less than the average FWHM of the stellar point-spread function on that frame. Differential magnitudes were computed with respect to the average of suitable comparison stars in the neighbourhood (± 300 pixels) of the target’s position and within -0.5 to $+1.5$ mag of its brightness. Calibrated magnitudes were determined by comparison to previously taken data or to the R_F magnitudes from the *Hubble Space Telescope* Guide Star Catalogue (GSC, Lasker et al. 2008) as provided by the ESO archive. The R_F passband differs significantly from the Bessel R filter curve, leading to systematic offsets between the two magnitudes depending on the spectral energy distribution of the object. From our comparison to several field stars, we estimate a typical uncertainty of ± 0.2 mag regarding this offset. We derive corresponding values for the V values for the comparison with earlier observations by correcting for the $V - R$ colour derived elsewhere. This introduces an additional uncertainty, because changes in brightness could well be accompanied by changes in colour (e.g., a brighter accretion disc is usually also bluer). However, with respect to the brightness differences observed in the present work and the previously reported colours of novae, e.g. by Szkody (1994) and (Zwitter & Munari 1995, 1996), we do not expect such change to exceed ~ 0.1 mag.

Reduction of the spectroscopic data consisted of the subtraction of the bias frame and the division by a flat-field that was normalized by fitting a high-order cubic spline to it. The spectra were extracted using the optimal extraction algorithm (Horne 1986) as implemented in IRAF’s ONEDSPEC package. Wavelength calibration was achieved with the data from HeAr lamps. The data were not flux calibrated, but a correction of the instrumental response function that was established from previous observations was applied to the grism #4 spectra, so that the continuum trend should be mostly reproduced correctly (the data were not taken at airmasses higher than 1.3).

2.2 Analysis

A large number of our objects show comparatively weak and broad emission lines. Additionally, due to the faintness of the objects and the necessarily short exposure times, the spectroscopic data have a low signal-to-noise ratio (S/N) typically not higher than ~ 10 . This presents significant difficulties for measuring the radial velocity displacement of the $H\alpha$ emission line by fitting a Gaussian function to it. We therefore adopt a different strategy by computing the average spectrum and iteratively shifting and scaling that spectrum until it yielded a visually reasonable fit to the individual spectra. This ‘eyeball cross-correlation’ has the disadvantage of being considerably more time-consuming, but it yields in general smoother radial velocity curves because the human eye can more easily ignore the influence of noise or additional emission components (e.g., Tappert et al. 2003) than a mathematical function. A few spectra (e.g. for AR Cir) that present more Gaussian line profiles and good S/N allowed for a comparison of the two methods, and we found the respective results to agree well with each other. Finally, to account for possible instrumental flexure, such determined radial velocities are corrected for the actual position of the [OI] $\lambda 6363.78$ Å night sky line.

The radial-velocity and light curves are examined for periodicities using the Scargle (1982) and analysis-of-variance (AOV; Schwarzenberg-Czerny 1989) algorithms as implemented in ESO-MIDAS (Warmels 1992). From our experience we find that the former is useful to restrict the range of possible periods, while the

Table 2. Radial velocity parameters as defined in equation (1).

Object	γ (km s $^{-1}$)	$K_{H\alpha}$ (km s $^{-1}$)	σ_{φ_0} (orbits)
V365 Car 2011	$-16(10)$	103(15)	0.021
V365 Car 2012	$-25(5)$	116(7)	0.010
AR Cir	21(3)	101(4)	0.006
V972 Oph 2011	$-3(4)$	115(7)	0.007
V972 Oph 2012	$-79(4)$	104(7)	0.007
HS Pup	85(4)	119(5)	0.006
V909 Sgr	$-117(11)$	109(15)	0.021
V373 Sct	55(5)	188(8)	0.005
CN Vel	7(5)	156(6)	0.008

latter more successfully suppresses alias periods within this range. The uncertainty of the selected period was estimated from the width of the peak in the Scargle periodogram, since their shape very roughly resembles a Gaussian, while the AOV peaks are more irregular.

The radial velocities are subsequently folded with the selected period and fitted with a sinusoidal function

$$v_r(\varphi) = \gamma - K_{H\alpha} \sin(\varphi - \varphi_0), \quad (1)$$

where γ is the constant term, $K_{H\alpha}$ the semi-amplitude and φ is the orbital phase with respect to φ_0 . The time of this zero-point of the orbital phase is determined either as the red-to-blue crossing of the radial velocity curve, and thus corresponds to the superior conjunction of the emission source, or with respect to orbital features (e.g., an eclipse) detected in the photometric light curve. The errors associated with these parameters have been estimated by the means of a Monte Carlo routine.

3 RESULTS

3.1 V365 Carinae = Nova Car 1948

This star was never observed ‘real time’ during its nova eruption. Its remnant was detected about 26 years after its outburst maximum during a search for emission line stars, assigning it the identification He 3-558 due to its $H\alpha$ emission. Henize & Liller (1975) noted that the spectrum of this object resembles that of an old nova, and carried out a search for variability in the Harvard plate archive. They detected that, in fact, it had erupted as a nova with a maximum photographic brightness $m_{pg} = 10.1$ mag in 1948 September 25 and a very slow decline afterwards ($t_3 = 530$ d according to Duerbeck 1987). Gill & O’Brien (1998) performed a search for a nova shell without success. In a spectrum taken in 1995, Zwitter & Munari (1996) find the Bowen/HeII emission blend to be significantly stronger than the Balmer emission lines, which they interpret as the signature of a rather hot white dwarf. The continuum, on the other hand, presents only a modest blue slope, but the authors speculate on this being due to interstellar reddening. They furthermore note the absence of HeI emission. The brightness at that time was $V = 18.31$ mag, thus yielding a comparatively small eruption amplitude $\Delta m \sim 8$ mag as expected from a slow nova (e.g., Duerbeck 1981). V365 Car was observed at the same brightness level by Woudt & Warner (2002), who performed high speed photometry during three nights in 2000 March for a total of 21 h. Their most extended runs present a hump-like wave structure with an amplitude of about 0.15 mag. They concluded that the corresponding period should be either 6.86 or 8.00 h. A slow flickering

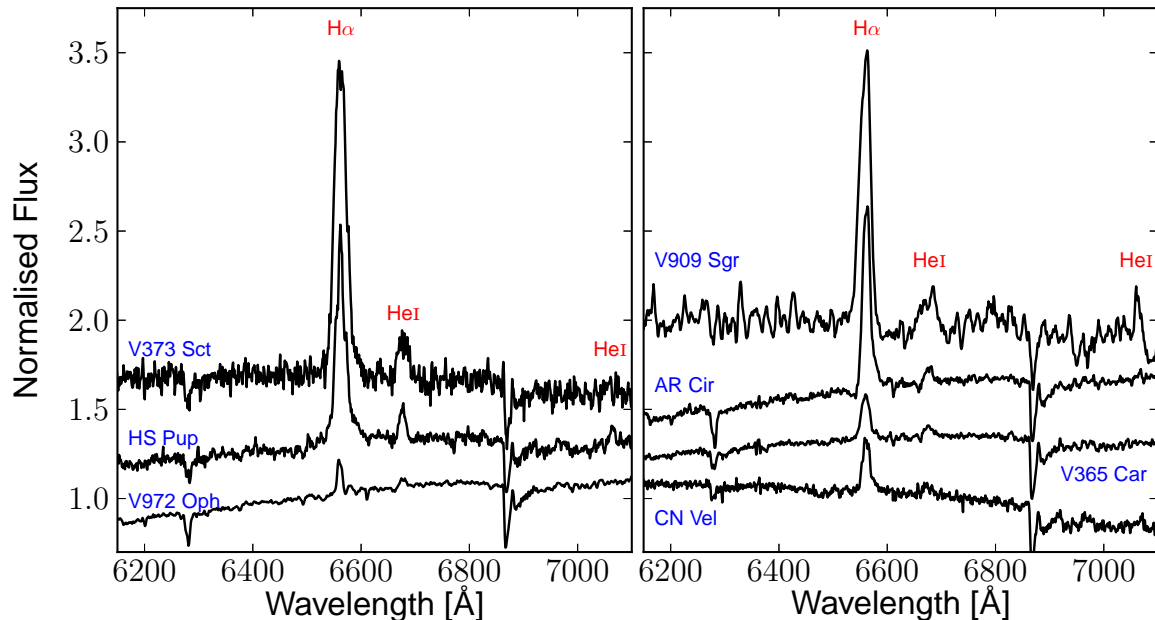


Figure 1. Average spectra for the seven novae as labelled. The spectra have been normalized by dividing through the mean flux and vertically displaced for display purposes. The V909 Sgr data have been smoothed with a 3×3 box filter.

with ~ 0.1 mag amplitude was also present. V365 Car is located near the outer border of the open cluster NGC 3532, but located beyond it, because the distance of this nova is of the order of 3.5 kpc, a factor 10 larger than that of the cluster (Henize & Liller 1975).

We observed V365 Car on three occasions, in 2011 February, 2012 March and May. Comparing the acquisition frames with the GSC we find as average values $R = 17.63(05)$, $17.67(06)$ and $17.68(06)$ mag for the runs in above sequence. The values in the parentheses here do not indicate a measurement uncertainty, but correspond to the mean variability. The 2012 runs thus show the object at the same brightness level, while it appears slightly brighter in the 2011 data. Zwitter & Munari (1996) give $V - R_C = 0.43$ mag for a Cousins R filter curve, yielding $V \sim 18.1$ mag for our data. Since the involved uncertainties amount to ~ 0.2 mag this does not necessarily mean that the object was in a (much) different brightness state than during the Zwitter & Munari (1996) and the Woudt & Warner (2002) observations.

The average spectrum, composed out of the data of all runs, is given in Fig. 1. The main feature is a comparatively weak $H\alpha$ line with an equivalent width $W_{H\alpha} = 5 \text{ \AA}^1$. We also note the presence of the HeI $\lambda 6678$ emission line that was not detected in the Zwitter & Munari (1996) spectrum. Looking at their data suggests that it was probably hidden by the low S/N and the lower spectral resolution.

The combined 2012 time-series photometric data from the acquisition frames yield a strong and unambiguous periodic signal at a frequency $f = 4.45 \text{ cycle d}^{-1}$ (top plot in Fig. 2). This peak is equally present in the combined 2012 radial velocities (although accompanied by an important alias at $5.45 \text{ cycle d}^{-1}$), while the 2011 data do not give any useful result due to the low S/N and insufficient sampling. Since folding the data according to above frequency yields reasonable curves for all data sets, we

identify this signal as corresponding to an orbital modulation at $P_{\text{orb}} = 0.2247(40) \text{ d} = 5.35(10) \text{ h}$.

In the middle plot of Fig. 2, we include the 2011 light-curve data (for clarity only one orbit is plotted) to show that these in general present the same modulation as the 2012 data, but are systematically offset to brighter magnitudes. The shape of the R light curve is that of a sinusoid or a hump with a semi-amplitude of $\Delta m_R \sim 0.1$ mag. The origin of the variation could therefore be either irradiation of the secondary star by the primary or the bright spot that is formed by the accretion stream from the secondary star hitting the accretion disc around the primary. The low amplitude, together with the stochastic variations caused by flickering, makes it impossible to distinguish between these two scenarios on the basis of our data, although the presence of flickering rather favours a bright-spot possibility. The zero-point of the radial-velocity curve defined as the superior conjunction of the emission source coincides with the minimum of the light curve. We use this zero-point to define the ephemeris of the variation as

$$T_0(\text{HJD}) = 245\,6067.4692(23) + 0.2247(40) E, \quad (2)$$

where E is the cycle number. The radial-velocity parameters are summarized in Table 2, the last column there giving the error associated with the determination of the zero-point φ_0 .

3.2 AR Circinis = Nova Cir 1906

Pickering (1907) announced the detection of this nova on Harvard patrol plates and gave a photographic maximum brightness $m_{\text{pg}} = 9.5$ mag. Duerbeck (1987) cites a number of references for the long-term light curve and derives $t_3 = 415 \text{ d}$. Duerbeck & Grebel (1993) reported the system to have a close visual K3V companion of $V = 14$ mag, with a separation of only 3.1 arcsec from AR Cir. A corresponding correction for the contribution of the companion of the nova eruption light curve yielded a maximum photographic magnitude 10.5, and the quiescent magnitudes and colours $V = 18.31$, $B - V = 1.25$ and $V - R = 1.0$. Like V365 Car, AR Cir is thus

¹ For convenience, we use here and throughout the paper positive values for W_λ . This is unambiguous since we exclusively refer to emission lines.

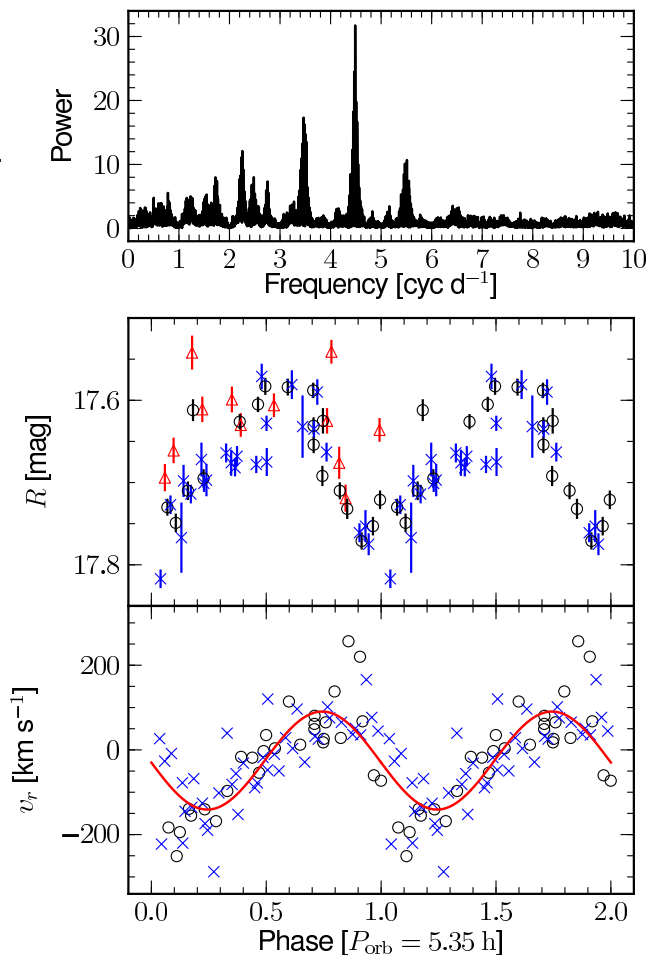


Figure 2. Time-series data on V365 Car. Top: AOV periodogram of the 2012 photometric data. Middle: light curves from 2011 February (triangles), 2012 March (circles) and May (x). Bottom: radial velocities from 2012 March (circles) and May (x).

a member of the novae that have a small eruption amplitude and show a slow decline. The spectrum taken by Duerbeck & Grebel (1993) shows a prominent $H\alpha$ emission line on a reddened continuum. Gill & O’Brien (1998) performed a search for a nova shell without success. The available infrared photometric data on AR Cir are erroneous, because the values obtained by Harrison (1992) refer to the combined light of the nova and its close visual neighbour, while Saito et al. (2013) measure only the latter (this will be corrected in the upcoming electronic version of the catalogue; Saito, private communication).

Because of the above mentioned source confusion, and because the Downes et al. (2005) catalogue lists the coordinates of the visual companion instead of the nova, we have measured accurate (to ~ 0.16 arcsec) coordinates from our acquisition frames using Starlink’s GAIA² tool (version 4.4.1) in combination with the UCAC3 (Zacharias et al. 2010) catalogue (see also Paper I). Such measured position is

$$\alpha_{2000.0} = 14:48:09.26, \quad \delta_{2000.0} = -60:00:24.8. \quad (3)$$

Fig. 3 presents the corresponding finding chart.

From our photometry we find a mean magnitude $R =$

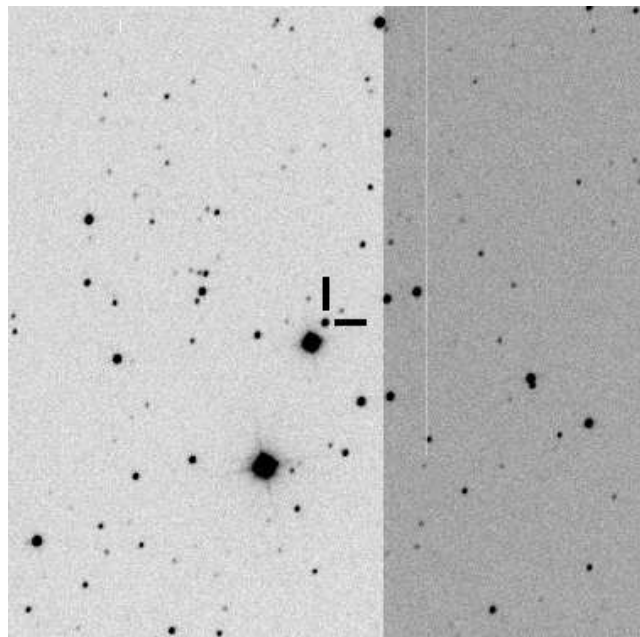


Figure 3. R -band finding chart for AR Cir. The size is 1.5×1.5 arcmin². North is up, east is to the left.

17.73(10) mag, with the value in the parentheses giving the mean variation. Taking $V - R = 1.0$ from Duerbeck & Grebel (1993) this yields $V \sim 18.7$. Taking into account the estimated uncertainty in our comparison to GSC magnitudes of ~ 0.2 mag, the object still can be suspected to be a few tenths of a magnitude fainter during our observations.

The average spectrum is given in Fig. 1. The $H\alpha$ emission line ($W_{H\alpha} = 19 \text{ \AA}$) and the HeI line at 6678 \AA (and to a lesser extent also 7065 \AA) can be clearly identified. In spite of the red continuum slope, the spectrum does not show any obvious absorption features from the secondary star. Consulting NASA’s Infrared Science Archive (IRSA) web interface that provides the interstellar extinction as measured by Schlegel, Finkbeiner, & Davis (1998), we find $E(B - V) = 5.3 \pm 0.3$ for AR Cir. This represents by far the largest reddening within our sample, and it is thus reasonable to assume that the observed red continuum is mainly due to reddening and does not represent the manifestation of the secondary star. Testing different values for the reddening we find that a correction for $E(B - V) \sim 2$ yields a similar continuum slope as for the other novae. A more precise measurement would require the analysis of interstellar absorption lines.

Applying the AOV algorithm to the radial velocities yields a peak corresponding to a period $P = 0.2143(72) \text{ d} = 5.14(17) \text{ h}$ (Fig. 4, top). The peak is comparatively broad due to the uneven sampling of the data, but folding the radial velocities on this period yields a smooth sinusoid with a standard deviation of $\sigma = 18 \text{ km s}^{-1}$ (Fig. 4, bottom). The parameters of the best fit to the data are given in Table 2. The R -band light curve shows a variation with a semi-amplitude of ~ 0.16 mag consisting of a broad maximum and a comparatively sharp minimum. This resembles a (partial) eclipse of the light source rather than an orbital hump or a sinusoidal variation. We use this minimum to define the ephemeris by computing a polynomial function of the second order to the eclipse shape, yielding

$$T_0(\text{HJD}) = 245\,6067.59969(06) + 0.2143(72) E. \quad (4)$$

² <http://astro.dur.ac.uk/~pdraper/gaia/gaia.html>

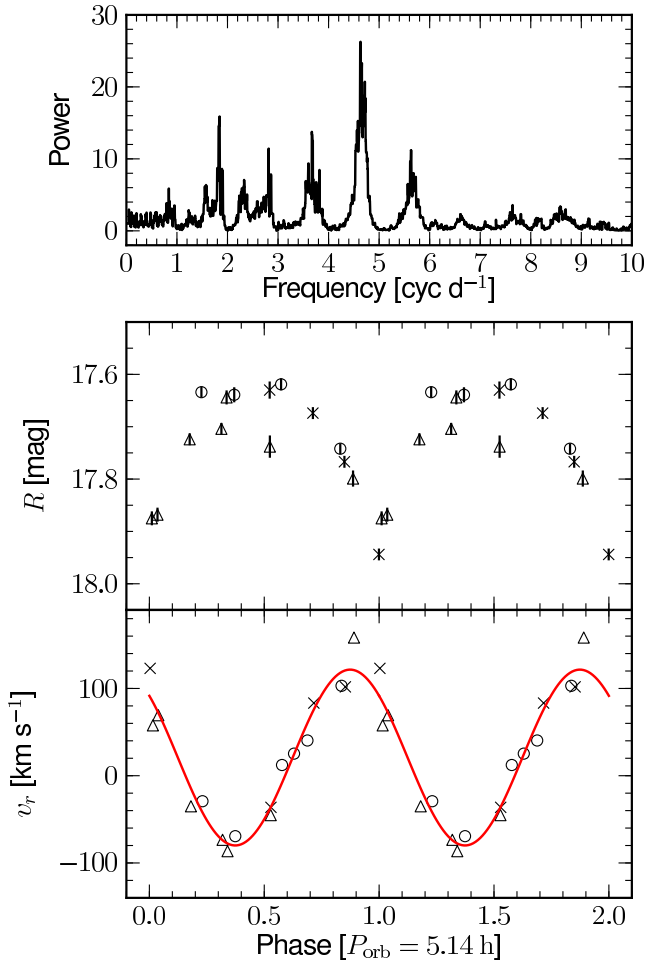


Figure 4. Time-series data on AR Cir. Top: AOV periodogram of the radial velocities. Middle: R light curve. Bottom: radial velocities. In the latter two, different symbols represent different nights.

The phase difference between the photometric minimum and the zero-point of the $H\alpha$ radial-velocity curve amounts to 0.12 orbits. Thus, in a coordinate system that has its point of origin in the centre-of-mass and whose axis connects the eclipsed continuum source (at 0°) with the eclipsing source (at 180°), the $H\alpha$ emission source is located at $\sim 43^\circ$ (clockwise). Identifying the eclipsing source with the secondary star implies a rather unusual location for the $H\alpha$ emitter. A bright spot, for example, would be expected at $\sim 135^\circ$. However, the bright-spot scenario is still possible if the accretion disc is small and the mass ratio is large so that the secondary star and the bright spot are on opposite sides of the centre-of-mass. To confirm this one would need radial velocities from the secondary star. If the disc indeed is small such should be obtainable with time-series infrared spectroscopy.

Finally, we find that the $H\alpha$ line profile shows an intriguing variability. In Fig. 5 we plot binned spectra (three spectra per bin with the exception of the bin corresponding to phase 0.21, which includes only two). We can identify four contributors to the $H\alpha$ line profile: the main component that makes up the base of the line and probably originates in the accretion disc, a narrow peak that moves within this base at slightly higher velocities and in CVs usually represents emission from the region of the bright spot or from the secondary star, a weak blue absorption component that is most pronounced in the spectra around phase 0.5, and finally a weak red

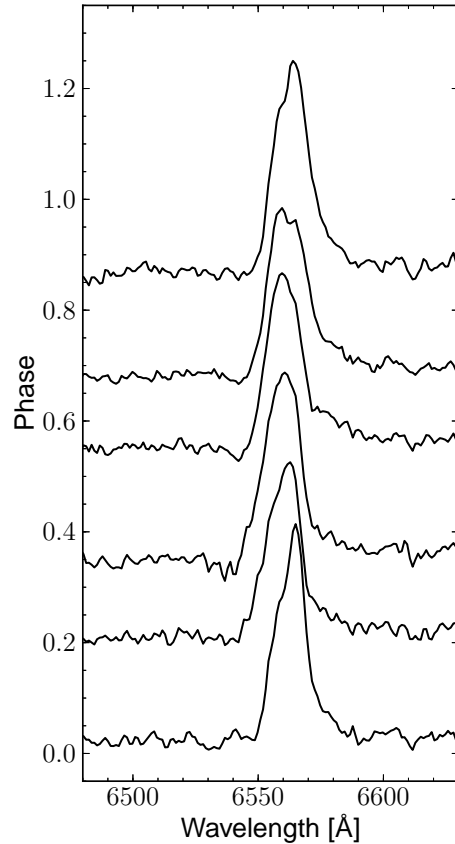


Figure 5. Binned spectra of AR Cir vertically offset according to orbital phase.

emission component that can be detected in all bins, but again is best visible at the same time as the absorption component. This simultaneous presence of a high-velocity blue absorption with a red emission counterpart indicates that these components represent redshifted and blueshifted $H\alpha$ caused by an optically thick wind or outflowing material similar to a P Cyg profile. Measuring the separation between the absorption and emission P Cyg component with a cursor yields a rough estimate of the (projected) outflow velocity to $700 \pm 100 \text{ km s}^{-1}$.

3.3 V972 Ophiuchi = Nova Oph 1957

Detected by Haro in 1957 on Tonantzintla plates (Haro & Whipple 1958), this nova reached $m_{\text{pg}} = 8.0$ mag at maximum. Duerbeck (1987) gives $t_3 = 176$ d and reports a pre-maximum halt of at least 50 d. Ringwald, Naylor, & Mukai (1996) present a continuum spectrum between 4000 and 10000 Å, with a single weak $H\alpha$ emission line, but with a rather strong continuum luminosity excess between 4000 and 5000 Å. This excess is not present in Zwitter & Munari (1996) who find a comparatively steep red continuum, strong HeII $\lambda 4686$ emission, $H\beta$ as a narrow emission line within an absorption trough, and $H\alpha$. The authors remark on the absence on HeI emission, and conclude that the system harbours a hot white dwarf, but in fact the HeI $\lambda 6678$ emission line is clearly present in their spectrum. Due to the absence of late-type absorption features they suggest that the companion has a spectral type F or earlier, requiring considerable interstellar extinction to explain the red continuum. Woudt, Warner, & Pretorius (2004) took high-speed photometry on three occasions for a total of 8.5 h. They find

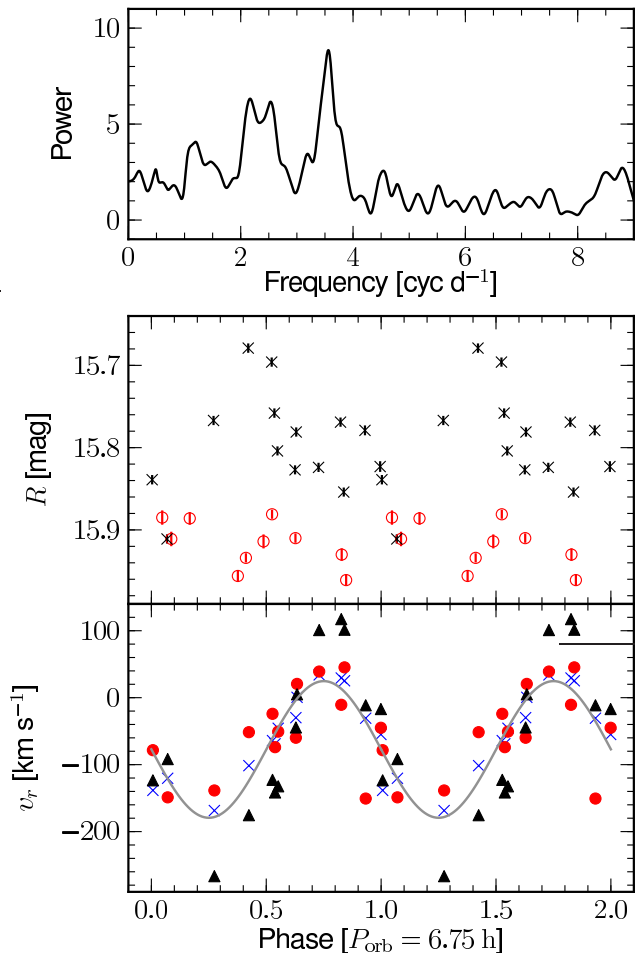


Figure 6. Time-series data on V972 Oph. Top: combined Scargle periodogram. Middle: R light curves from 2011 June/July (circles) and from 2012 May (\times). Bottom: radial velocities of the $H\alpha$ line (\times), its additional emission component (triangles), and the line tentatively identified as CII (circles). The sine represents the best fit to the $H\alpha$ data.

some flickering activity with a maximum amplitude of 0.1 mag at a time-scale of about 15 min, but no longer periodic modulation. The two available infrared studies (2MASS and VVV, Hoard et al. 2002; Saito et al. 2013, respectively) differ by about 4 mag. A comparison of the coordinates shows that the Two Micron All Sky Survey (2MASS) data are the correct ones, while the object is misidentified in the VVV. V972 Oph appears to show some long-term low-amplitude variations: Ringwald et al. (1996) report $V = 16.7$ mag in 1991 mid-June; Zwitter & Munari (1996) find the star at $V = 16.56$ mag in 1994 April 18; and Woudt et al. (2004) measure $V = 15.9$ mag in 2002 April 2, $V = 16.1$ mag in 2003 August 29 and $V = 16.2$ mag one night later.

We observed the system on two occasions: on two nights in 2011 June/July and on four consecutive nights in 2012 May (Table 1). From comparison of the acquisition frames with the GSC we find that the object on average was slightly brighter during the 2012 run, with $R \sim 15.8$ mag, than on the 2011 run, with $R \sim 15.9$ mag. Ringwald et al. (1996) and Zwitter & Munari (1996) measured similar colours, $V - R = 0.7$ mag and 0.63 mag, respectively. For our data, this yields $V \sim 16.5$ and ~ 16.6 mag. This suggests that V972 Oph was in a brightness state close to that during the

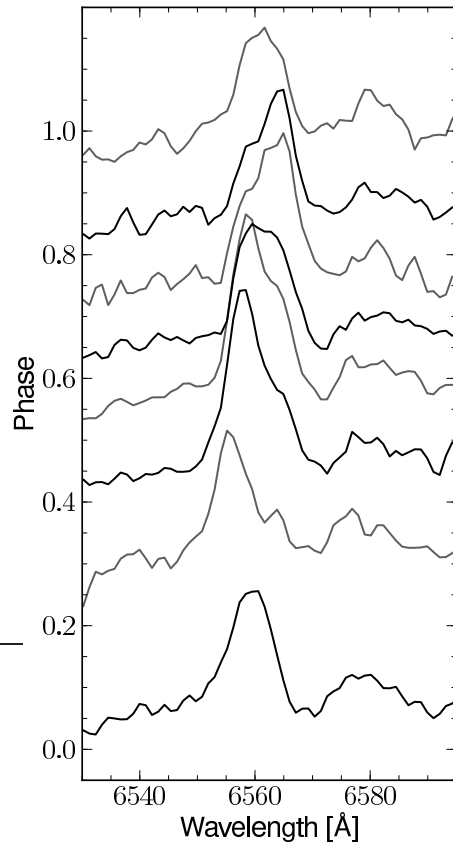


Figure 7. Close-up of the spectral region around $H\alpha$ plotted versus orbital phase for V972 Oph. Spectra within the same 0.1 orbits wide phase bins have been averaged.

two studies above, and slightly fainter than during the observations by Woudt et al. (2004).

The time span between the two runs is too large to combine the data for a time-series analysis, so the sets had to be analysed individually. The periodograms in each case present two significantly strong peaks, but only the one at $f = 3.558$ cycle d^{-1} is common to both sets (Fig. 6, top). Folding the data with this frequency yields a smooth sine curve (Fig. 6, bottom), and we thus identify the modulation with an orbital one corresponding to a period $P_{\text{orb}} = 0.281(8)$ d = 6.75(19) h. Sine fits to the radial velocities yield the parameter collected in Table 2. Defining the zero-points of the phase as the time of the red-to-blue crossing of the radial-velocity curves yields the ephemeris

$$T_0(\text{HJD}) = 245\,5744.719(02) + 0.281(8) E \quad (5)$$

for the 2011 June/July set, and

$$T_0(\text{HJD}) = 245\,6067.749(02) + 0.281(8) E \quad (6)$$

for the 2012 May set. As we will discuss below, there are significant differences in the light curves of the two runs that could in principle also affect the profile of the emission line. The two ephemerides thus do not necessarily correspond to the same physical zero-point of the orbital motion.

The average spectrum shows a peculiar broad line centred at ~ 6580 Å. The line moves approximately parallel with the $H\alpha$ line; a sine fit to its radial velocity yields a semi-amplitude $K_{6580} = 78(11)$ km s^{-1} , which is $\sim 2.4 \sigma$ lower than $K_{H\alpha}$, and a phase difference of 0.04(02) orbits for the 2012 May data (Fig. 6, bot-

tom). For comparison, for the He I $\lambda 6678$ emission line we find $K_{6678} = 119(9) \text{ km s}^{-1}$ and a phase difference of 0.06(01). We can discard the possibility that the two lines in reality form one broad H α line that is split by an absorption component, because the bluer line of the two clearly shows the presence of an additional component that moves within that blue line and never crosses over to the red one. In fact, some of the phase-binned spectra shown in Fig. 7 hint at a corresponding emission component being present in the red line. The blue line thus necessarily must be H α . The identity of the red line is less clear. Because it shows the same orbital motion as the other lines it can not be a forbidden line originating in a shell, e.g. [N II] $\lambda 6584^3$. Examining the identification list of lines in stellar spectra (Coluzzi 1999) we find as the most likely possibility that the line represents the C II $\lambda\lambda 6578/6583$ doublet. Carbon emission lines have been observed previously, e.g. in the post-novae V840 Oph (Schmidtobreick et al. 2003) and CP Pup (Bianchini et al. 2012). However, both these systems show considerable C and He II emission in the blue ($<6000 \text{ \AA}$) wavelength range, which does not appear to be the case in V972 Oph, although the available blue spectra (Zwitter & Munari 1996; Ringwald et al. 1996) have low S/N and/or low spectral resolution and can thus provide no concluding evidence. Additionally, strong C II $\lambda\lambda 6578/6583$ emission has been reported for the helium nova V445 Pup in the first few months after eruption, but there they are clearly related to the outflow (Wagner et al. 2001; Iijima & Nakanishi 2008). We note that the separation between the suspected C II line and H α in velocity units amounts to $\sim 700 \text{ km s}^{-1}$, i.e. the same as the suspected outflow in AR Cir (Section 3.2). However, in V972 Oph we do not find any evidence for an accompanying blue absorption or emission component⁴. Considering the weakness of the H α emission it seems unlikely that such an absorption component could be hidden in its wings.

Folding the photometric R data on the spectroscopic period shows that, in spite of the small offset of ~ 0.1 mag in average magnitude between the 2011 data and the 2012 data, the light curves present significantly different shapes that are likely to reflect structural difference at the time of the two observing runs (Fig. 6). The 2011 light curve is the slightly fainter one and is reminiscent of an ellipsoidal variation with minima at spectroscopic phases ~ 0.3 and ~ 0.9 . In contrast, the 2012 data show a hump at phase ~ 0.5 and a minimum at ~ 0.1 orbits. The latter, however, is defined by only one data point and therefore has to be treated with some caution. Additionally, one has to take into account that both data sets have been folded with respect to their individual spectroscopic ephemeris, and as remarked above these do not necessarily refer to the same orbital configuration.

With the available data it is not possible to say if the differences in the photometric behaviour are also reflected in the line emission distribution. The 2011 spectra have much lower S/N and are more affected by fringing, so that an examination of the line profile does not provide further information. The average spectra, at least, show identical line strengths (e.g., $W_{\text{H}\alpha} \sim 2 \text{ \AA}$ in both cases).

³ An additional argument against this possibility is that the shell was not detected in H α /[N II] imaging conducted by Gill & O’Brien (1998).

⁴ As can be seen in the average spectrum in Fig. 1 there is an absorption line at $\sim 6530 \text{ \AA}$, but apart from having about twice the separation from H α as the suspected C II emission, it also does not show any detectable velocity variations and is thus probably of interstellar origin.

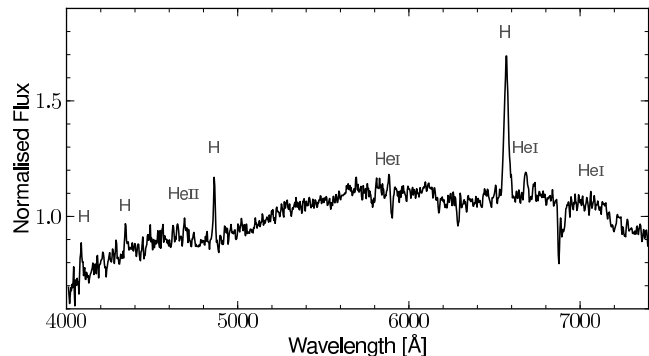


Figure 8. Normalized low-resolution spectrum of HS Pup. Positions of typical emission lines are indicated by corresponding labels.

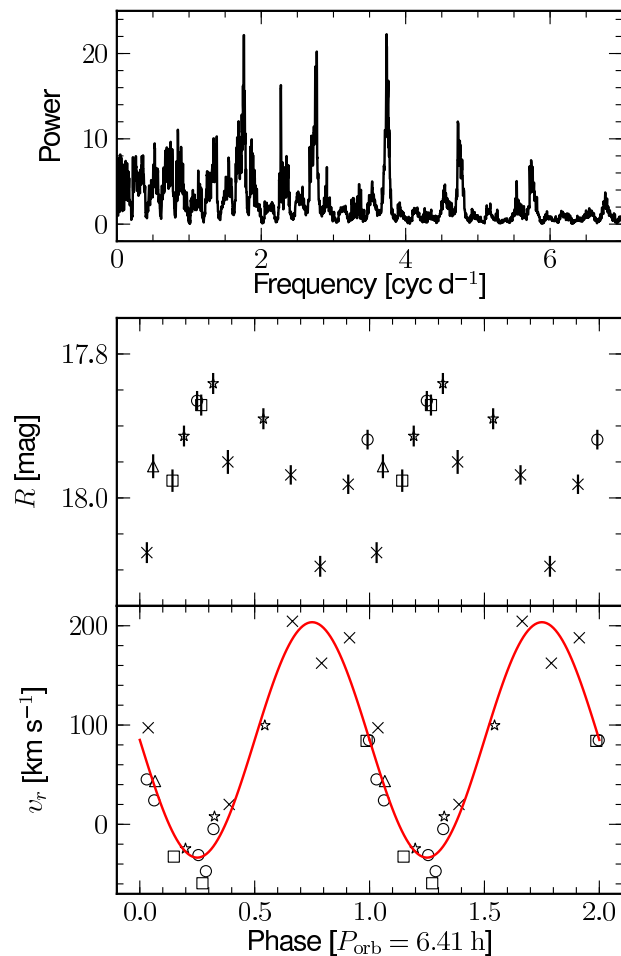


Figure 9. Time-series data on HS Pup. Top: AOV periodogram of the radial velocities of the H α peak component. Middle: R light curve. Bottom: radial velocities of the H α peak component. The sine represents the best fit. In the latter two plots, different symbols indicate different nights.

3.4 HS Puppis = Nova Pup 1963

Discovered by Strohmeier (1964) on plates of the Bamberg Southern Station, it reached maximum on 1963 December 23 ($m_{\text{pg}} = 8.0$ mag). In spite of its southern position, its light curve could be monitored from the Sonneberg observatory until 1964 February (Huth & Hoffmeister 1964). Duerbeck (1987) classifies it as a moderately fast nova with a decay time $t_3 = 65 \text{ d}$. Gill & O’Brien

(1998) detect a shell around HS Pup with a diameter of <2.5 arcsec. An optical spectrum can be found in Zwitter & Munari (1995). As a single feature it presents a weak but rather broad and potentially double-peaked $H\alpha$ emission line. Infrared magnitudes can be found in Hoard et al. (2002). A time-series photometric study was conducted by Woudt & Warner (2010). They find strong flickering activity at time-scales of 15 min and amplitudes up to 0.15 mag. From a very weak periodic signal they suggest a possible orbital modulation with a period of 3.244 h and an amplitude $\Delta V = 0.0161$ mag. Like many old novae, HS Pup undergoes low-amplitude long-term variations: Szkody (1994) observed it in 1989 April at $V = 18.06$ mag and Woudt & Warner (2010) found it at $V = 17.8$ mag in 2000 December and 2001 February, as well as at $V = 18.0$ mag in 2008 January. The only larger deviation is reported by Zwitter & Munari (1995) who measured $V = 19.1$ mag from a spectrum taken in 1994 October.

The low-resolution spectrum shown in Fig. 8 represents an average of 12 spectra that were taken in 2009 May, with the system being at $R \sim 17.6$ mag (Table 1). In spite of measuring different V magnitudes, Szkody (1994) and Zwitter & Munari (1995) report very similar colours of $V - R = 0.38$ and 0.40 mag, respectively. This yields $V \sim 18.0$ for our spectrum. The much improved S/N with respect to the previously available data allows us to detect the full series of Balmer emission lines, as well as the presence of HeI. Notable is the weakness or even absence of the Bowen/HeII $\lambda 4686$ complex that usually is one of the signatures of old novae. This suggests that the mass-transfer rate in HS Pup is lower than in other post-novae. Comparison with standard stars from several libraries (Jacoby, Hunter, & Christian 1984; Pickles 1985; Silva & Cornell 1992) shows that the red part of the continuum agrees well with that of an early to mid K star, indicating a comparatively long orbital period.

Analysis of the radial velocities measured in spectra taken in 2011 February/March indeed suggests several possible periods longward of 6 h: $P_1 = 6.41$ h, $P_2 = 8.72$ h and $P_3 = 13.75$ h (Fig. 9, top). Folding the data on these periods yields a significantly better fit for P_1 than for the other two. An additional point in favour of P_1 is that it is approximately twice the photometric period detected by Woudt & Warner (2010). We thus conclude that the orbital period of HS Pup is $P_{\text{orb}} = 0.2671(38)$ d = 6.41(09) h. Defining the point of the red-to-blue crossing of the radial velocity curve as the zero-point of the orbital phase yields the ephemeris to

$$T_0(\text{HJD}) = 245\,5624.7071(17) + 0.2671(38) E. \quad (7)$$

The parameters corresponding to the best sine fit of the data are given in Table 2. Using this sine fit within the framework of the time-series analysis shows that the other peaks in the periodogram are aliases corresponding to the window function.

R magnitudes measured from the acquisition frames indicate that the system was about 0.3–0.4 mag fainter than for the 2009 spectrum. This is also reflected in the emission lines. For the average 2011 spectrum we measure the equivalent width of $H\alpha$ to $W_{H\alpha} = 25$ Å, while in 2009 the line was slightly weaker ($W_{H\alpha} = 17$ Å). Folding the R magnitudes on the spectroscopic period yields a light curve that is roughly consistent with an orbital modulation in the form of a sinusoidal variation with an amplitude of ~ 0.25 mag. The apparent presence of flickering, however, makes it necessary to average a much larger number of measurements to analyse the shape of the light curve in detail.

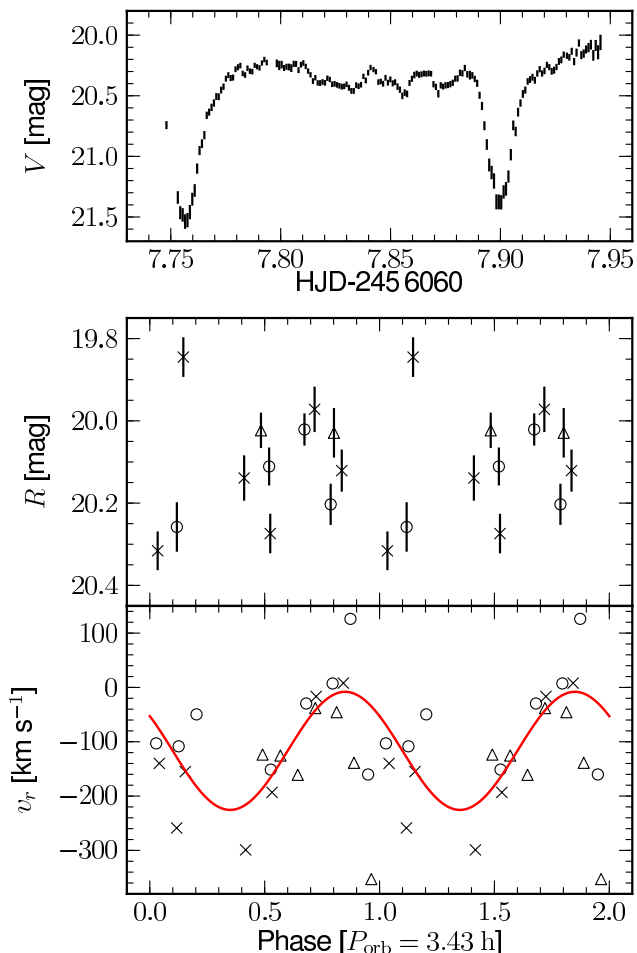


Figure 10. Time-series data on V909 Sgr. Top: V light curve. Middle: R light curve. Bottom: radial velocities of the $H\alpha$ peak component. The sine represents the best fit. In the latter two plots different symbols indicate different nights.

3.5 V909 Sagittarii = Nova Sgr 1941

A brief history of this very fast nova ($t_3 = 7$ d; Duerbeck 1987) is included in Paper I. The spectrum presented there shows strong HeII contribution indicating a magnetic system, as already suspected by Diaz & Bruch (1997). The latter authors furthermore report the system to be eclipsing with an approximate period of 3.36 h, but stated the need for confirmation.

Due to the faintness of the target the radial velocities of the $H\alpha$ emission line proved very difficult to measure, in spite of the considerable strength of the line (Fig. 1; $W_\lambda = 41$ Å). We have therefore additionally taken a V -band light curve and were fortunate to cover two eclipses with our data (Fig. 10, top). We measure the times of the minima of the two eclipses to HJD 245 6067.75640(72) and HJD 245 6067.89926(55). This yields the orbital period to $P_{\text{orb}} = 0.14286(17)$ d = 3.4286(41) h, which corrects the preliminary value from Diaz & Bruch (1997) by about four minutes. The formal ephemeris is thus

$$T_0(\text{HJD}) = 245\,6067.89926(55) + 0.14286(17) E. \quad (8)$$

Note that the error estimation here does not take into account potential influences of the timings by long-term changes. The two here recorded eclipses, e.g., differ by ~ 0.15 mag in depth. A longer time series would thus be desirable to improve the statistics.

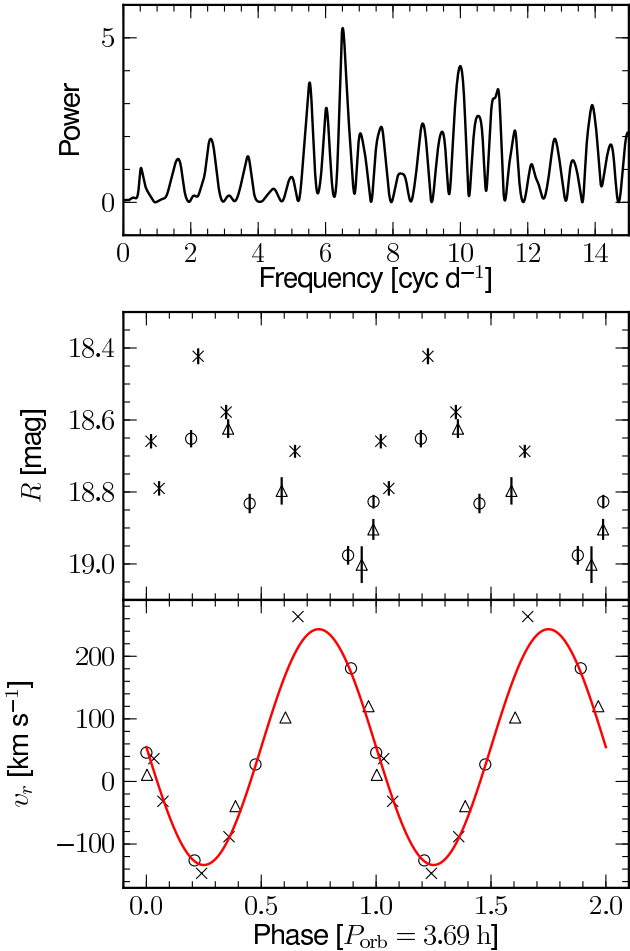


Figure 11. Time-series data on V373 Sct. Top: Scargle periodogram of the H α radial velocities. Middle: R light curve. Bottom: radial velocities of the H α line. The sine represents the best fit to the data. In the latter two plots, different symbols indicate different nights.

Both the R magnitudes from the acquisition frames and the H α radial velocities show considerable noise when folded on above ephemeris. A sine fit to the radial-velocity data yields the parameters summarized in Table 2. The zero-point of the radial-velocity curve coincides with a photometric phase of 0.10(02), indicating that the source of the emission is approximately on the opposite side from the centre-of-mass as seen from the secondary star.

Finally we briefly remark on the presence of a previously unidentified eclipsing variable star in the field of V909 Sgr. Its coordinates are RA_{2000.0} = 18:25:52.34, Dec_{2000.0} = -35:03:05.4 with an uncertainty of 0.25 arcsec. The average magnitude is $V = 18.7$ mag and the light curve is reminiscent of a W UMa star. In our 4.74 h light curve we cover one eclipse and one maximum, the two having a brightness difference of $\Delta V = 1.04$ mag. We determine the time of mid-eclipse to HJD 245 6067.799(03). The time difference between the two features is 2.45(10) h, so that the orbital period should be close to 9.8 h if the light curve is symmetric. This is a rather typical value for contact binaries (e.g., Rucinski 1992).

3.6 V373 Scuti = Nova Sct 1975

This moderately slow nova was discovered by Wild (1975) at the Zimmerwald Observatory, Switzerland. Its eruption light-curve

properties have been discussed by Strope, Schaefer, & Henden (2010) who assigned it subtype J with a decay time $t_3 = 79$ d and a maximum magnitude $V = 6.1$. The subtype J (jitter) refers to post-maximum isolated flare-ups of the order of 1 mag. In V373 Sct, these are observed only within the first ~ 150 d after eruption. An optical spectrum of the post-nova taken by Ringwald et al. (1996) shows strong Balmer emission and an equally strong Bowen/HeII $\lambda 4686$ component. Woudt & Warner (2003) performed high-speed photometry of V373 Sct, finding strong flickering activity at time-scales of 15 min and amplitudes up to 0.6 mag. They also found a coherent oscillation in one of their runs with a period of 258.6 s and suggest that V373 Sct might belong to the DQ Her type class of intermediate polars, with a rapid, non-synchronous rotation of the white dwarf.

Our observations of V373 Sct cover three consecutive nights from 2011 June 29 to July 1 (Table 1). The average spectrum (Fig. 1) presents a strong H α emission line with an equivalent width $W_\lambda = 53$ Å, which is slightly below the value of 57 Å recorded by Ringwald et al. (1996). Using their colour $V - R = 0.3$ mag, our R magnitudes translate to $V \sim 18.4$ mag. Thus, the system was slightly brighter than in the Ringwald et al. (1996) data ($V = 18.7$ mag), which fits well with the weaker H α emission. Additionally, the spectrum shows the clear presence of HeI $\lambda 6678$ and also a hint of very weak HeI $\lambda 7065$.

Analysis of the radial velocities of the H α emission line yields several possible alias peaks (Fig. 11, top), but only the highest one at $f = 6.51$ cycle d⁻¹ gives an acceptable radial-velocity curve. We thus identify this peak with the orbital period $P_{\text{orb}} = 0.1536(28)$ d = 3.69(07) h. The ephemeris corresponding to the time of red-to-blue crossing results to

$$T_0(\text{HJD}) = 245\,5744.8376(10) + 0.1536(28) E. \quad (9)$$

Fitting the radial velocities with a sine function yields an unusually large semi-amplitude $K_{\text{H}\alpha} = 188$ km s⁻¹ (Fig. 11, bottom; Table 2). Consequently, the emission source has to be situated comparatively far away from the centre-of-mass, with a distance of

$$a_{\text{H}\alpha} \sin i = K_{\text{H}\alpha} P_{\text{orb}} / 2\pi \sim 0.57 R_\odot \quad (10)$$

representing a lower limit. At an orbital period below 4 h thus either the system has a comparatively high mass ratio, or the main contributor to the H α emission is (close to) the secondary star. In any case the inclination of the system should be comparatively high. This is reflected in the R light curve that shows a variation with an amplitude of about 0.6 mag (Fig. 11, middle). At first glance the light curve appears to have an unusual sawtooth shape with a short and steep rise and a slow decline. However, the incompleteness of the phase coverage leaves room for the possibility of an ellipsoidal shape with two minima of different depth at 0.5 and 0.9 orbits and two maxima of different height at phases 0.2 and 0.7. Additionally, with the small number of data points the potential presence of flickering (that had been observed in the V filter by Woudt & Warner 2003) can distort the light curve significantly.

3.7 CN Velorum = Nova Vel 1905

This very slow nova was discovered by Leavitt on Harvard plates (Leavitt & Pickering 1906). Peaking at $m_{\text{pg}} = 10.2$ mag, the decay time was $t_3 > 800$ d (Duerbeck 1987). A spectrum of the post-nova is included in Zwitter & Munari (1996). It shows a noisy blue continuum with a weak H α emission line.

Our low-resolution spectrum in Fig. 12 presents a bit more

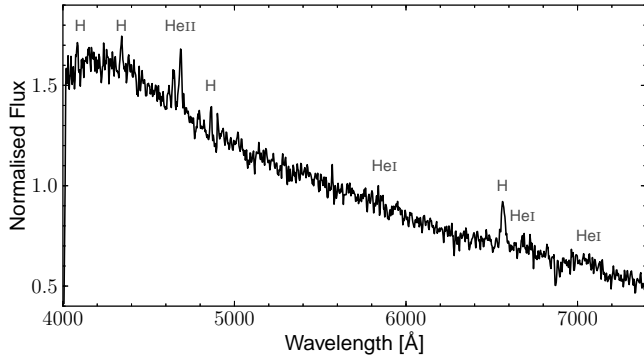


Figure 12. Normalized low-resolution spectrum of CN Vel. Positions of typical emission lines are indicated by corresponding labels.

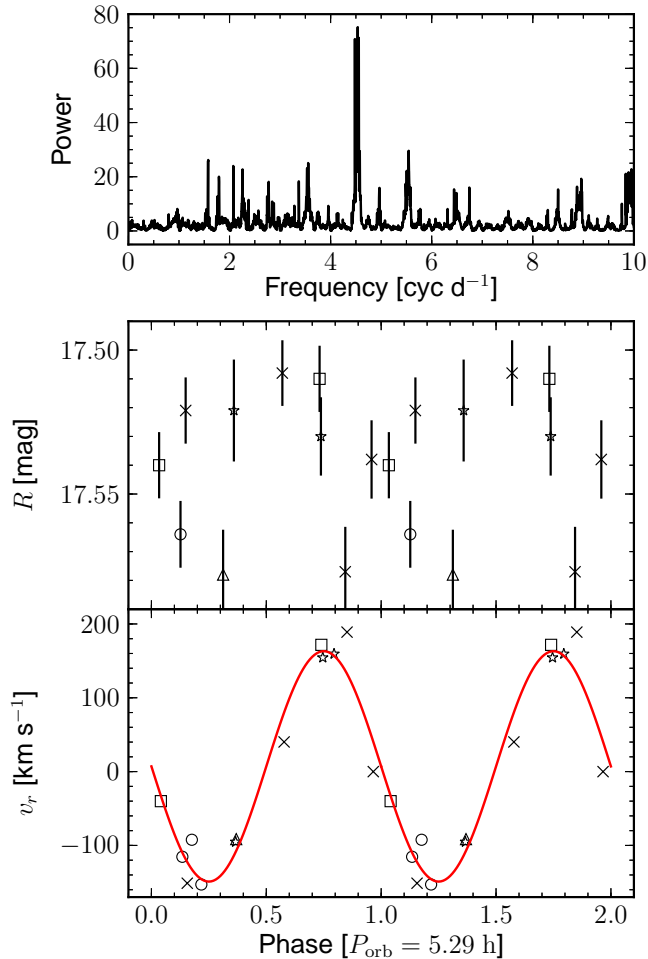


Figure 13. Time-series data on CN Vel. Top: AOV periodogram of the $H\alpha$ radial velocities. Middle: R light curve. Bottom: radial velocities of the $H\alpha$ line. The sine represents the best fit to the data. In the latter two plots different symbols indicate different nights.

detail. Apart from the Balmer series and a few weak HeI emission lines the Bowen/HeII $\lambda\lambda 4650/4686$ component appears particularly strong. Together with the steep blue continuum this indicates that this post-nova is still maintaining a high mass-transfer rate.

Analysis of the radial velocities gives an unambiguous signal at $f = 4.55$ cycle d^{-1} (Fig. 13, top) which we identify with the orbital period $P_{\text{orb}} = 0.2202(30)$ d = 5.285(72) h. As with V373

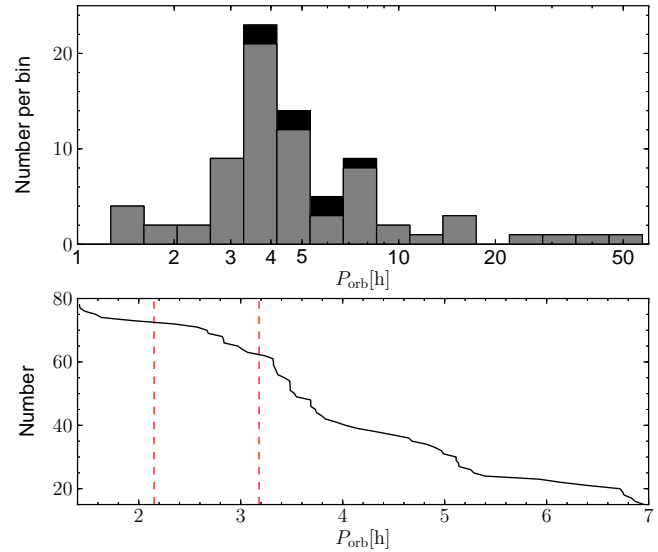


Figure 14. Top: observed period distribution of classical novae on a logarithmic scale. The data are from the Ritter & Kolb (2003) catalogue (grey) and the present paper (black). Bottom: the cumulative distribution for periods 1.4–7.0 h. The dashed lines mark the limits of the period gap from Knigge (2006).

Sct, the amplitude of the radial-velocity curve is comparatively high (Fig. 13, bottom; Table 2), which suggests that a significant amount of the $H\alpha$ emission originates close to the secondary star. Defining the ephemeris by the means of the red-to-blue crossing of the radial-velocity curve yields

$$T_0(\text{HJD}) = 245\,5624.8533(17) + 0.2202(30) E. \quad (11)$$

In contrast to all the other systems in our sample, the photometric R -band data of CN Vel do not appear to be modulated with the spectroscopic period (Fig. 13, middle). However, we have seen that slow low-amplitude photometric variations in post-novae are a common phenomenon. In principle it could be possible that the system was in a slightly lower state on the first nights of our observations, 2011 February 19 and 21. Excluding these two data points (the circle and the triangle) the remaining data appear consistent with a sinusoidal signal of an amplitude of ~ 0.06 mag. Note that this is based on a mere assumption and needs confirmation by further observations. The uncertainties of our photometric measurements are certainly large enough to allow for any kind of variability or even none at all. Zwitter & Munari (1996) measured $V = 17.78$ mag and $V - R = 0.16$ mag for their observations. Applying their colour to our data yields $V \sim 17.7$ mag and thus a similar brightness.

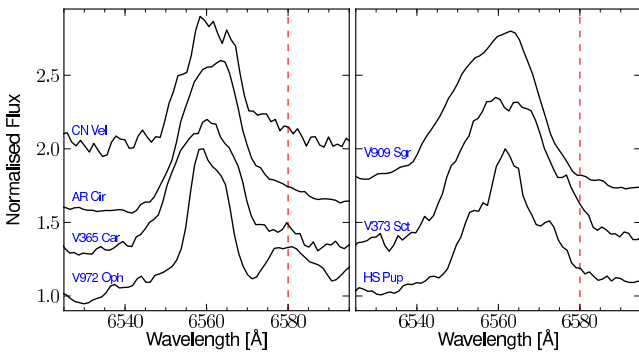
CN Vel has a close visual neighbour, and while the finding chart in the Downes et al. (2005) catalogue is unambiguous, the listed coordinates refer to the combined light. We have measured the position of the nova on an R -band image as described for AR Cir in Section 3.2 to

$$\alpha_{2000.0} = 11:02:38.66, \quad \delta_{2000.0} = -54:23:09.5 \quad (12)$$

with a precision of $\sigma = 0.18$ arcseconds.

Table 3. Properties of the novae.

Object	Year	t_3 (d)	Δm (mag)	P_{orb} (h)	$W_{\text{H}\alpha}$ (Å)
V909 Sgr	1941	7	13.5	3.43	41
V373 Sct	1975	79	12.6	3.69	53
AR Cir	1906	415	8.2	5.14	19
CN Vel	1905	>800	7.5	5.29	5
V365 Car	1948	530	8.0	5.35	5
HS Pup	1963	65	10.0	6.41	25
V972 Oph	1957	176	8.5	6.75	2

**Figure 15.** $\text{H}\alpha$ line profiles of the average spectra that have been normalized with respect to the maximum intensity of the line. The spectra have been displaced vertically for display purpose. The dashed line marks the position of C II .

4 DISCUSSION AND CONCLUSION

In the top plot of Fig. 14 we present the updated period distribution on a logarithmic scale⁵ using the data from Ritter & Kolb (2003, update 7.20, 2013 June), limiting the set to Galactic classical novae with unambiguous orbital periods, but including the probable prehistoric novae Z Cam and AT Cnc (Shara et al. 2007, 2012b, respectively), to yield a total number of 71 orbital periods. The addition of the results of the present work thus represents an increase of about 10 per cent, which emphasizes the undersampling of the observed distribution. Following the measurement of the edges of the period gap to 2.15 and 3.18 h by Knigge (2006), we can dissect the period distribution into selected bins. We find that there are 6 systems (corresponding to 8 per cent) below the period gap and 10 (13 per cent) in the gap, with the large majority of systems occupying the range above the period gap, but only 14 novae (18 per cent) with $P_{\text{orb}} > 7$ h. The fraction of novae in the 3–4 h range is 31 per cent and thus less than the ~ 50 per cent predicted by Townsley & Bildsten (2005), and only two of our new additions fall into this regime. However, the cumulative distribution (Fig. 14, bottom) still shows that the slope from ~ 3.8 – 3.2 h is about a factor of 4 steeper than for other period ranges, proving that this bin is overpopulated. The vast majority of CVs in this period range have been identified as SW Sex stars (Rodríguez-Gil et al. 2007b), systems whose characteristics indicate that they have very high \dot{M} (Rodríguez-Gil, Schmidtobreick, & Gänsicke 2007a). This is thus in agreement with the general idea of the importance of this param-

eter for nova eruptions. It is furthermore confirmed that the slope within the period gap is only slightly lower than e.g. the range from 5 to 4 h, i.e. there is a significant number of novae in the period gap. Townsley & Bildsten (2005) argue that these should contain a magnetic white dwarf, in which case the interaction of the magnetic field with the secondary star could prevent magnetic braking to operate (Li, Wu, & Wickramasinghe 1994). Evidence, albeit not always conclusive, for the presence of a magnetic white dwarf has been found for V4633 Sgr (Lipkin & Leibowitz 2008), V351 Pup (Woudt & Warner 2001), V630 Sgr (Schmidtobreick et al. 2005), V2214 Oph (Baptista et al. 1993), V597 Pup (Warner & Woudt 2009), V Per (Wood, Abbott, & Shafer 1992) and DD Cir (Woudt & Warner 2003), i.e. for seven of the 10 novae in the gap. This exceeds the estimated fraction of ~ 22 per cent of magnetic CVs (Araujo-Betancor et al. 2005) by far, and thus provides strong support for above hypothesis.

In Table 3, we present selected properties of our novae. The year of the eruption gives us the time Δt that has passed from the eruption to our current observations, and thus the ‘age’ of the post-nova. Next is the time t_3 in which the nova has declined by 3 mag from maximum brightness. The values were mostly taken from Duerbeck (1987) and in one case (V373 Sct) from Strope et al. (2010). Column 3 gives the eruption amplitude Δm which has been calculated as the difference between the reported maximum brightness and the average V magnitudes of the post-nova. For the calculation of the latter we have included our own measurements as well as data from the literature. Because the maximum magnitudes are not corrected for the colour difference between V and the (mostly) photographic plates the involved uncertainties can well be within the 0.5 mag range. In spite of these uncertainties, our sample seems to present well the general behaviour of post-novae in the Δm versus $\log t_3$ diagram, when considering all 11 novae contained in Paper I (table 5) and in Table 3 here. Within the expected scatter, they are in perfect agreement with the linear relation given in equation (1) of Vogt (1990), based on a much larger sample of post-novae. Column 4 gives the orbital period P_{orb} and column 5 gives the equivalent width $W_{\text{H}\alpha}$ of the $\text{H}\alpha$ emission line, which shows a rough inverse dependency on \dot{M} (Patterson 1984). Note, however, that such correlation is only valid if the majority of the $\text{H}\alpha$ emission originates in the accretion disc and is thus indicative of its brightness. In our sample we find two systems, where this is not the case: V909 Sgr, which is a probable magnetic system, and HS Pup, whose line profile shows a much stronger contribution of an additional component than in the other systems (Fig. 15).

In Section 3.3, we have reported on the probable detection of the $\text{C II } \lambda\lambda 6578, 6583$ doublet in emission. Carbon emission is a common feature in the ultraviolet spectra of CVs (e.g., La Dous 1991), and as part of the Bowen blend at $\lambda 4640$ Å in high \dot{M} CVs (e.g., Williams 1983). Additionally, a few CVs show enhanced carbon emission, mainly in the blue part of their spectra (e.g., Drew et al. 2003; Schmidtobreick et al. 2003; Bianchini et al. 2012). The carbon content in CVs and pre-CVs is a potential indicator of the evolutionary status of the binary and especially the secondary star, which has motivated several corresponding studies (Gänsicke et al. 2003; Harrison, Osborne, & Howell 2004, 2005a; Harrison et al. 2005b; Tappert et al. 2007; Howell et al. 2010; Hamilton et al. 2011). However, to our knowledge this particular C II emission has never been observed before in a CV with the exception of V445 Pup, where it originates in the expelled nova shell (Iijima & Nakanishi 2008), while in V972 Oph it is clearly situated in the binary itself. A favourable factor in its detection is certainly the comparatively narrow and weak $\text{H}\alpha$ emission line. This

⁵ The bin size is given by $\Delta P = 10^{(n+1)/10} - 10^{n/10}$ h, where $n = 0, 1, 2, \dots$

raises the question if the presence of (perhaps slightly weaker) CII in other CVs is not simply masked by the typically broad and strong H α line. In Fig. 15, we compare the line profiles of the seven novae. To account for the different line strengths we have normalized the spectra with respect to the maximum intensity of the line. On the left-hand side of the plot we have collected the ‘carbon suspects’, i.e. the novae that show a certain extra flux near 6580 Å. Apart from V972 Oph these are V365 Car, AR Cir and CN Vel. The line profiles of the remaining three novae in the right-hand plot of the figure show more symmetric wings, although the line in V373 Sct is certainly sufficiently broad to hide potentially present weak CII. The inclusion of AR Cir in this list demonstrates that a red extended H α emission wing can also indicate the presence of an outflow rather than CII emission. Considering that evidence for such outflow has been detected for several CVs in ultraviolet lines (e.g., Froning 2005) but also in H α and HeI (Kafka & Honeycutt 2004), this represents perhaps an even more likely explanation. Additionally, the outflow phenomenon in CVs appears to be most commonly found in systems with high \dot{M} and most post-novae certainly fall into that category. However, assuming that such outflows are bipolar (Drew 1987) we would then expect to find a blueshifted counterpart either in absorption (for an optically thick outflow) or in emission (for an optically thin outflow as has been recently detected in VY Scl; Schmidtobreick et al., MNRAS, submitted). Apart from AR Cir, in none of the other targets any such component can be detected in our data, but on the other hand a (weak) absorption component could be easily masked by the principal H α emission line.

The data presented here were obtained with the intention to determine the orbital periods of the seven novae, and they served this purpose well. A closer inspection reveals interesting phenomena in a number of systems, but the limited quality of the data mostly allows only a glimpse at them and often raises more question than answers. Several of the novae here merit further investigation, and we hope that the present work motivates more detailed studies.

ACKNOWLEDGEMENTS

We thank Elena Mason and Antonio Bianchini for discussion on the spectrum of V972 Oph and Roberto Saito for comments regarding the VVV infrared data on several novae.

This research was supported by FONDECYT Regular grant 1120338 (CT and NV). AE acknowledges support by the Spanish Plan Nacional de Astronomía y Astrofísica under grant AYA2011-29517-C03-01.

We gratefully acknowledge ample use of the SIMBAD data base, operated at CDS, Strasbourg, France, and of NASA’s Astrophysics Data System Bibliographic Services. IRAF is distributed by the National Optical Astronomy Observatories.

REFERENCES

Araujo-Betancor S., Gänsicke B. T., Long K. S., Beuermann K., de Martino D., Sion E. M., Szkody P., 2005, *ApJ*, 622, 589
 Baptista R., Jablonski F. J., Cieslinski D., Steiner J. E., 1993, *ApJ*, 406, L67
 Bianchini A., Saygac T., Orío M., Della Valle M., Williams R., 2012, *A&A*, 539, A94
 Coluzzi R., 1999, *VizieR Online Data Catalog*, 6071
 de Kool M., 1992, *A&A*, 261, 188

Diaz M. P., Bruch A., 1997, *A&A*, 322, 807
 Downes R. A., Webbink R. F., Shara M. M., Ritter H., Kolb U., Duerbeck H. W., 2005, *J. Astron. Data*, 11, 2
 Drew J. E., 1987, *MNRAS*, 224, 595
 Drew J. E., Hartley L. E., Long K. S., van der Walt J., 2003, *MNRAS*, 338, 401
 Duerbeck H. W., 1981, *PASP*, 93, 165
 Duerbeck H. W., 1987, *Space Sci. Rev.*, 45, 1
 Duerbeck H. W., Grebel E. K., 1993, *MNRAS*, 265, L9
 Eckert W., Hofstadt D., Melnick J., 1989, *The Messenger*, 57, 66
 Froning C. S., 2005, in Hameury J.-M., Lasota J.-P., eds, *ASP Conf. Ser. Vol. 330, The Astrophysics of Cataclysmic Variables and Related Objects*, Astron. Soc. Pac., San Francisco, p.81
 Gänsicke B. T. et al., 2003, *ApJ*, 594, 443
 Gänsicke B. T. et al., 2009, *MNRAS*, 397, 2170
 Gill C. D., O’Brien T. J., 1998, *MNRAS*, 300, 221
 Hamilton R. T., Harrison T. E., Tappert C., Howell S. B., 2011, *ApJ*, 728, 16
 Haro G., Whipple F., 1958, *Harvard College Observatory Announcement Card*, 1405, 1
 Harrison T. E., 1992, *MNRAS*, 259, 17P
 Harrison T. E., Osborne H. L., Howell S. B., 2004, *AJ*, 127, 3493
 Harrison T. E., Osborne H. L., Howell S. B., 2005a, *AJ*, 129, 2400
 Harrison T. E., Howell S. B., Szkody P., Cordova F. A., 2005b, *ApJ*, 632, L123
 Henize K. G., Liller W., 1975, *ApJ*, 200, 694
 Hoard D. W., Wachter S., Clark L. L., Bowers T. P., 2002, *ApJ*, 565, 511
 Horne K., 1986, *PASP*, 98, 609
 Howell S. B., Harrison T. E., Szkody P., Silvestri N. M., 2010, *AJ*, 139, 1771
 Huth H., Hoffmeister C., 1964, *Inf. Bull. Var. Stars*, 60, 1
 Iijima T., Nakanishi H., 2008, *A&A*, 482, 865
 Jacoby G. H., Hunter D. A., Christian C. A., 1984, *ApJS*, 56, 257
 Kafka S., Honeycutt R. K., 2004, *AJ*, 128, 2420
 King A. R., 1988, *Q. J. R. Astron. Soc.*, 29, 1
 Knigge C., 2006, *MNRAS*, 373, 484
 La Dous C., 1991, *A&A*, 252, 100
 Lasker B. M. et al., 2008, *AJ*, 136, 735
 Lasota J.-P., 2001, *New Astron. Rev.*, 45, 449
 Leavitt H. S., Pickering E. C., 1906, *Harvard College Observatory Circular*, 121, 1
 Li J. K., Wu K. W., Wickramasinghe D. T., 1994, *MNRAS*, 268, 61
 Lipkin Y. M., Leibowitz E. M., 2008, *MNRAS*, 387, 289
 Nelson L. A., MacCannell K. A., Dubeau E., 2004, *ApJ*, 602, 938
 Patterson J., 1984, *ApJS*, 54, 443
 Pickering E. C., 1907, *Astron. Nachr.*, 175, 333
 Pickles A. J., 1985, *ApJS*, 59, 33
 Rappaport S., Verbunt F., Joss P. C., 1983, *ApJ*, 275, 713
 Retter A., Leibowitz E. M., Kovo-Kariti O., 1998, *MNRAS*, 293, 145
 Ringwald F. A., Naylor T., Mukai K., 1996, *MNRAS*, 281, 192
 Ritter H., Kolb U., 2003, *A&A*, 404, 301
 Rodríguez-Gil P., Schmidtobreick L., Gänsicke B. T., 2007a, *MNRAS*, 374, 1359
 Rodríguez-Gil P. et al., 2007b, *MNRAS*, 377, 1747
 Rucinski S. M., 1992, *AJ*, 103, 960
 Saito R. K. et al., 2013, *A&A*, 554, A123
 Scargle J. D., 1982, *ApJ*, 263, 835
 Schlegel D. J., Finkbeiner D. P., Davis M., 1998, *ApJ*, 500, 525

- Schmidtobreick L., Tappert C., Bianchini A., Mennickent R. E., 2003, *A&A*, 410, 943
- Schmidtobreick L., Tappert C., Bianchini A., Mennickent R. E., 2005, *A&A*, 432, 199
- Schwarzenberg-Czerny A., 1989, *MNRAS*, 241, 153
- Shara M. M. et al., 2007, *Nature*, 446, 159
- Shara M. M., Mizusawa T., Zurek D., Martin C. D., Neill J. D., Seibert M., 2012a, *ApJ*, 756, 107
- Shara M. M., Mizusawa T., Wehinger P., Zurek D., Martin C. D., Neill J. D., Forster K., Seibert M., 2012b, *ApJ*, 758, 121
- Silva D. R., Cornell M. E., 1992, *ApJS*, 81, 865
- Starrfield S., Sparks W. M., Truran J. W., 1976, in Eggleton P., Mitton S., Whelan J., eds, *Proc. IAU Symp. 73, Structure and Evolution of Close Binary Systems*, Reidel, Dordrecht, p.155
- Stehle R., Kolb U., Ritter H., 1997, *A&A*, 320, 136
- Stetson P. B., 1992, in Worrall D. M., Biemesderfer C., Barnes J., eds, *ASP Conf. Ser. Vol. 25, Astronomical Data Analysis Software and Systems I*, Astron. Soc. Pac., San Francisco, p.297
- Strohmeier W., 1964, *Inf. Bull. Var. Stars*, 59, 1
- Strope R. J., Schaefer B. E., Henden A. A., 2010, *AJ*, 140, 34
- Szkody P., 1994, *AJ*, 108, 639
- Tappert C., Mennickent R. E., Arenas J., Matsumoto K., Hanuschik R. W., 2003, in Sterken C., ed., *ASP Conf. Ser. Vol. 292, Interplay of Periodic, Cyclic and Stochastic Variability in Selected Areas of the H-R Diagram*, p.413
- Tappert C., Gänsicke B. T., Schmidtobreick L., Mennickent R. E., Navarrete F. P., 2007, *A&A*, 475, 575
- Tappert C., Ederoclite A., Mennickent R. E., Schmidtobreick L., Vogt N., 2012, *MNRAS*, 423, 2476 (Paper I)
- Tappert C., Vogt N., Schmidtobreick L., Ederoclite A., Vanderbeke J., 2013, *MNRAS*, 431, 92 (Paper II)
- Townsley D. M., Bildsten L., 2004, *ApJ*, 600, 390
- Townsley D. M., Bildsten L., 2005, *ApJ*, 628, 395
- Townsley D. M., Gänsicke B. T., 2009, *ApJ*, 693, 1007
- Vogt N., 1990, *ApJ*, 356, 609
- Wagner R. M., Schwarz G., Starrfield S. G., Foltz C. B., Howell S., Szkody P., 2001, *IAU Circ.*, 7717, 2
- Warmels R. H., 1992, in Worrall D. M., Biemesderfer C., Barnes J., eds, *ASP Conf. Ser. Vol. 25, Astronomical Data Analysis Software and Systems I*, Astron. Soc. Pac., San Francisco, p.115
- Warner B., Woudt P. A., 2009, *MNRAS*, 397, 979
- Wild P., 1975, *IAU Circ.*, 2791, 1
- Williams G., 1983, *ApJS*, 53, 523
- Wood J. H., Abbott T. M. C., Shafter A. W., 1992, *ApJ*, 393, 729
- Woudt P. A., Warner B., 2001, *MNRAS*, 328, 159
- Woudt P. A., Warner B., 2002, *MNRAS*, 335, 44
- Woudt P. A., Warner B., 2003, *MNRAS*, 340, 1011
- Woudt P. A., Warner B., 2010, *MNRAS*, 403, 398
- Woudt P. A., Warner B., Pretorius M. L., 2004, *MNRAS*, 351, 1015
- Zacharias N. et al., 2010, *AJ*, 139, 2184
- Zorotovic M., Schreiber M. R., Gänsicke B. T., 2011, *A&A*, 536, A42
- Zwitter T., Munari U., 1995, *A&AS*, 114, 575
- Zwitter T., Munari U., 1996, *A&AS*, 117, 449